

DOI: 10.1002/cphc.200500484

# Field Effect of Screened Charges: Electrical Detection of Peptides and Proteins by a Thin-Film Resistor

Simon Q. Lud,<sup>[a]</sup> Michael G. Nikolaides,<sup>[a]</sup> Ilka Haase,<sup>[b]</sup> Markus Fischer,<sup>[b]</sup> and Andreas R. Bausch<sup>\*[a]</sup>

For many biotechnological applications the label-free detection of biomolecular interactions is becoming of outstanding importance. In this Article we report the direct electrical detection of small peptides and proteins by their intrinsic charges using a biofunctionalized thin-film resistor. The label-free selective and quantitative detection of small peptides and proteins is achieved using hydrophobized silicon-on-insulator (SOI) substrates functionalized with lipid membranes that incorporate metal-chelating lipids. The response of the nanometer-thin conducting silicon film

to electrolyte screening effects is taken into account to determine quantitatively the charges of peptides. It is even possible to detect peptides with a single charge and to distinguish single charge variations of the analytes even in physiological electrolyte solutions. As the device is based on standard semiconductor technologies, parallelization and miniaturization of the SOI-based biosensor is achievable by standard CMOS technologies and thus a promising basis for high-throughput screening or biotechnological applications.

For many biotechnological applications, the label-free detection of biomolecular interactions is becoming significantly important. Herein, we report the direct electrical detection of small peptides and proteins by their intrinsic charges using a biofunctionalized thin-film resistor. The label-free selective and quantitative detection of small peptides and proteins is achieved using hydrophobized silicon-on-insulator (SOI) substrates functionalized with lipid membranes that incorporate metal-chelating lipids. The response of the nanometer thin conducting silicon film to electrolyte screening effects is taken into account to determine quantitatively the charges of peptides. It is even possible to detect peptides with a single charge, and to distinguish single charge variations of the analytes, even in physiological electrolyte solutions. As the device is based on standard semiconductor technologies, parallelization and miniaturization of the SOI-based biosensor is easily achievable by standard complementary metal oxide semiconductor (CMOS) technologies, and is thus a promising basis for high throughput screening or biotechnological applications.

Biosciences rely increasingly on the simultaneous and quantitative detection of a large number of biomolecular interactions. For the emerging field of system biology, miniaturized, parallel, and quantitative detection methods of protein interactions or DNA hybridizations are critical.<sup>[1]</sup> Furthermore, for biomedical and pharmaceutical research, detecting the interaction of small molecules or peptides with membranes or membrane proteins is becoming increasingly important.<sup>[2,3]</sup> Most state-of-the-art detection methods currently employed are based on the labeling of the analytes with fluorophores, chemiluminescent, or redox markers to detect their specific interactions with immobilized receptor molecules. However, these methods can be problematic, because labeling is an additional step in

sample preparation and can alter the overall structure of the analyte in a way that may affect its binding behavior. The modification of a ligand with a detectable marker molecule has long been known to be responsible for measuring artifacts, thus complicating quantitative measurements.<sup>[4]</sup> Label-free detections are thus highly desirable, and several approaches, based on the detection of the mass or binding induced mechanical distortions, have been introduced.<sup>[5–7]</sup>

The direct electrical detection of intrinsic charges of biomolecules with biofunctionalized semiconductor devices is also a promising approach, which would circumvent the obstacles of labeling; miniaturization could even allow the detection on single-cell levels.<sup>[1]</sup> To distinguish between different ligands or biomolecules, determining quantitatively the amount of charge per molecule is very important. The field effect at the electrolyte–insulator interface of semiconducting devices can be used to determine small surface potential variations evoked from the binding of charged molecules. In a common ion-selective field-effect transistor (ISFET), field-induced variations of the charge carrier concentrations near the surface of a semiconductor are detected by variations of a reference potential. This approach is normally used to detect pH changes evoked

[a] S. Q. Lud, Dr. M. G. Nikolaides, Prof. Dr. A. R. Bausch  
Lehrstuhl für Biophysik—E22  
Technische Universität München  
James Franck Str. 1  
85747 Garching (Germany)  
Fax: (+) 49-89-2891-2469  
E-mail: abausch@ph.tum.de

[b] Dr. I. Haase, Priv.-Doz. Dr. M. Fischer  
Lehrstuhl für Organische Chemie und Biochemie  
Technische Universität München (Germany)

by enzymatic activities, but it has rarely been used to detect biomolecules directly in a quantitative manner.<sup>[8]</sup>

The screening of charges in electrolyte solutions is a major obstacle for detecting the intrinsic charges of biomolecules. Recently, low-ionic-strength solutions or distilled water were used to detect DNA hybridization, antibody binding, and viruses by their intrinsic charge.<sup>[9–13]</sup> For small molecules, the binding can be assumed to occur close to the surface, and thus screening effects by the electrolyte solutions can be neglected.<sup>[11–14]</sup> However, the binding of proteins or small molecules at complex biofunctionalized surfaces occurs at a further distance from the surface, and results in a change of the surface charge inside the solution. Therefore, screening effects have to be taken into account in order to relate quantitatively the charges of the molecules and the change in the conductivity of the devices. Accounting for screening effects is also mandatory for understanding the sensitivity limitations of field-effect devices. As the biological activity of proteins and binding constants of ligand receptor systems rely on salt concentrations and defined pH, it is mandatory to first develop field-effect devices that enable the detection of even small charged molecules in these conditions, and secondly to understand how screening in the electrolyte solution will affect the solvent–insulator–semiconductor interface. Despite the importance of field-effect devices for the successful application of biosensing in research or diagnostics, screening effects have not yet been addressed.

As a promising material for biosensing applications, functionalized silicon nanowires are currently used to detect the specific binding of streptavidin, DNA hybridization, and viruses.<sup>[10,14,15]</sup> Although there are emerging concepts for the parallelization and functionalization of the nanowires,<sup>[10,16]</sup> sensor concepts based on planar substrates would have great technological advantages for all possible biotechnological applications. A conducting film, only a few nanometers thick, of a SOI substrate could be a promising candidate for building planar biosensing devices by standard semiconductor technologies.

Here, we demonstrate that nanometer thin-film resistors, based on SOI and functionalized by biomimetic lipid membranes, can detect small peptides with single charges, and distinguish even single charge variations between them.

The principle of the biosensing device is shown in Figure 1. The 30-nm-thick conducting silicon layer of the SOI substrate was structured by standard lithography. The native oxide surface was passivated by covalent coupling of a silane layer to the SiO<sub>2</sub> surface. Subsequently, the sensor device was functionalized by the solvent-exchange method with a lipid monolayer. Variations of the sheet resistance were determined in four-point geometry utilizing a Hallbar: A current was applied between the source and drain, and the voltage drop between two adjacent contacts was measured continuously. Calibration measurements in electrolyte solutions using an Ag/AgCl reference electrode were used to relate the surface potential of the passivated sensor device to the sheet resistance. The sensor and the reference electrodes were mounted into a microfluidic chamber, ensuring flow conditions for a rapid exchange of analytes at the interface.<sup>[17]</sup>

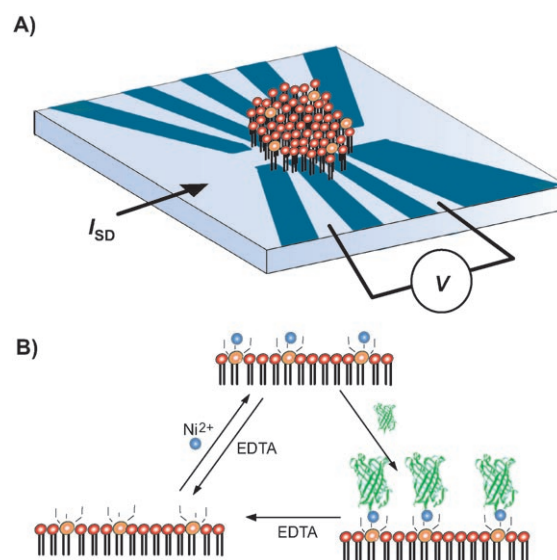


**Figure 1.** Schematic of the sensor device. A) A SOI substrate is structured with a Hallbar and functionalized with a lipid monolayer. The SiO<sub>2</sub> surface is silanized with octadecyltrimethoxysilane and covered with a 1,2-dimyristoyl-sn-glycero-3-phosphocholine, cholesterol and a 1,2-dioleoyl-sn-glycero-3-[[N(5-amino-1-carboxypentyl) iminodiacetic acid]succinyl DOGS-NTA monolayer by solvent exchange. B) The incorporated NTA lipids allow the specific coupling of histidine-tagged proteins or peptides to the membrane. Coupling only occurs if Ni<sup>2+</sup> is bound to the NTA headgroup. The Ni<sup>2+</sup> and thus the proteins can be unbound by competitive scavenging of Ni<sup>2+</sup> by ethylenediaminetetraacetic acid (EDTA).

Solid-supported fluid membranes have proven to be a robust and flexible system mimicking biological recognition processes at cellular membranes.<sup>[18,19]</sup> One promising concept for the reversible and specific coupling of proteins to biomimetic membranes is the incorporation of metal-chelating lipids into solid-supported membranes. A now widely used system is based on coupling 1,2-dioleoyl-sn-glycero-3-[[N(5-amino-1-carboxypentyl) iminodiacetic acid]succinyl (DOGS-NTA) headgroups to different lipids.<sup>[20]</sup> As shown in Figure 1 B, the configuration and electrostatic charge of the NTA headgroups are changed, owing to the binding of divalent nickel ions. Polyhistidine tags specifically bind to Ni<sup>2+</sup>-charged NTA headgroups, forming a noncovalent complex. As in most cases, the N- or C-terminal modification of proteins with polyhistidine tags causes only a minor impact on the folding pattern or the biochemical function. This approach is commonly used for protein purification. The unbinding of a polyhistidine peptide can be achieved by the addition of a strong chelator for Ni<sup>2+</sup>, such as ethylenediaminetetraacetic acid (EDTA). This process is reversible, and the activation of the sensor for further measurements can be facilitated just by again raising the Ni<sup>2+</sup> concentration. Biofunctionalization of the sensor device was achieved by depositing a lipid membrane, composed of DOGS-NTA lipids incorporated into a matrix of 1,2-dimyristoyl-sn-glycero-3-phosphocholine DMPC and cholesterol, onto the silanized interface.<sup>[21]</sup>

Small peptides with a defined number of charges and uniform charge distributions were used to elucidate the sensors sensitivity to small charge variations in small molecules. We

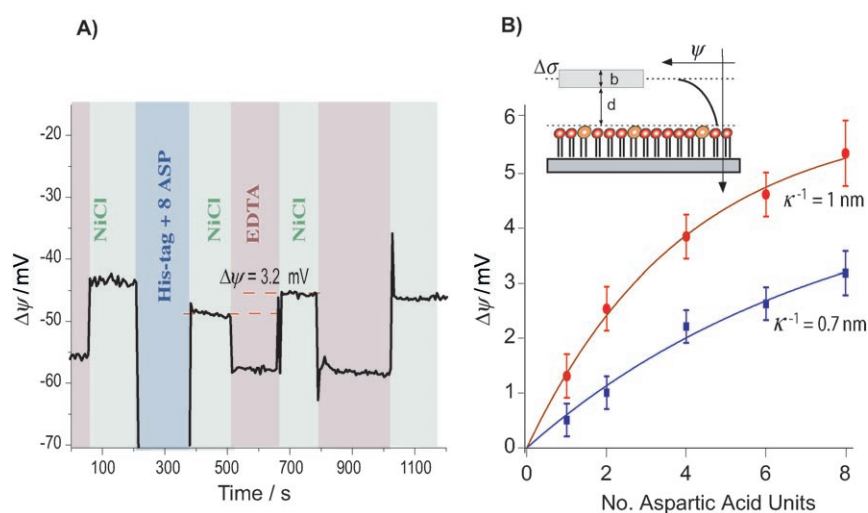


**Figure 2.** The binding of small peptides to the lipid monolayer was detected by the device. A) Once the NTA headgroups of the membrane are loaded with  $\text{Ni}^{++}$ , a buffer containing polyhistidine-tagged peptides is flushed through the sample chamber. The effect of the peptide binding on the surface potential was detected by subsequent exchange with the  $\text{Ni}^{++}$ -containing buffer. Unbinding of the peptides was achieved with an EDTA (50 mM) containing buffer, recovering the original surface potential. The binding of the peptide was thus specific and reversible. B) An increasing number of charged residues results in a bigger shift in the surface potential  $\Delta\psi$ . The nonlinear dependence can be attributed to screening effects in the electrolyte solution. At lower salt concentrations (red data points,  $\kappa^{-1}=1.1$  nm), a bigger sensor response and a bigger effective mean distance of the charges can be observed than for the higher salt concentrations (blue data points,  $\kappa^{-1}=0.7$  nm). The shown fits of Equation (1) result in a mean distance of  $d=2.8$  nm and a thickness of the charged layer  $b$  by 0.3 nm per charged residue at low salt concentrations. The results obtained at the higher salt concentrations were fitted with  $d=2.3$  nm and an increase in  $b$  by 0.1 nm per charged residue.

used hexahistidine tagged (Histag) peptides with different numbers of charged residues (aspartic acid), varying from a single-charged residue up to eight charged residues (His6Asp1 to His6Asp8). The binding of a single Histag-aspartic acid residue was clearly detected by the sensor (Figure 2). First, the NTA lipids were loaded with  $\text{Ni}^{++}$ , which can be observed by an increase in the surface potential ( $\psi$ ). The subsequent unbinding of  $\text{Ni}^{++}$  was achieved by washing with an EDTA-containing solution. Once the functional lipid headgroups were reloaded with  $\text{Ni}^{++}$  by washing with the standard  $\text{Ni}^{++}$  buffer, a solution containing 7  $\mu\text{M}$  of peptide was applied to the sensor device. Upon binding of the peptides, the surface potential in presence of the standard  $\text{Ni}^{++}$  buffer shifts, as can be seen in Figure 2A. The application of an EDTA solution unbinds the peptides and allows the original surface potential to recover. This demonstrates the specificity and reversibility of the binding and detection. An artificial hexamer of histidine residues, which is uncharged at pH 7.5, evoked no sensor response. In membranes without NTA lipids incorporated, no binding of His-tagged peptides was observed. The sensitivity of the sensor is high enough to distinguish between peptides with one or two charged residues (Figure 2B). Peptides with additional charged residues also result in distinct sensor signals. The surface-potential shift is based on the number of charged amino acids, that is, peptides with higher charges result in an increased sensor response. However, the measured signal for each additional charged amino acid decreases with increasing number of amino acids (Figure 2B). This behavior is attributa-

ble to the increased length of the peptide and the resulting increase in screening effect of the electrolyte solution.

To a first approximation, the bound peptides can be assumed to be a homogenous charge density located at an average distance  $d$  from the surface and to be smeared out over an average thickness  $b$ . The simple Debye–Hückel approximation for a smeared-out charge can be used to relate the change in the surface potential per area to the binding of the peptides, Equation (1):

$$\Delta\psi = \frac{\Delta\sigma}{b} \frac{[e^{-\kappa d} - e^{-\kappa(d+b)}]}{\epsilon_0 \epsilon_r \kappa^2} \quad (1)$$

where  $\epsilon_0$  is the dielectric constant,  $\epsilon_r$  is the permittivity of water and  $\kappa^{-1}$  is the Debye screening length. As the surface density of the DOGS-NTA lipids (5%) and the approximate headgroup area (0.65  $\text{m}^2$ ) are known, the discrete charges of the

bound peptide molecules can be approximated as a homogenous charge density  $\sigma$ , given by the number of charges per peptide molecule ( $z=1,2,4,6$ , and 8) times the number density of DOGS-NTA lipids  $\Delta\sigma = ze^{-}/65 \text{ \AA}^2 \times 5\%$ , assuming full surface coverage owing to the high binding affinity of the NTA-HisTag system.<sup>[22,23]</sup> This model follows from the symmetrical Green's function at solid interfaces and has been shown to hold for charges near surfaces.<sup>[24]</sup> Inserting the values of  $\epsilon_r=80$  and  $1/\kappa=1.1$  nm, an effective average distance of the peptide charges from the lipid headgroups can be thus determined by fitting Equation (1) to the experimental data. The mean distance  $d$  was determined by the length of the complete NTA headgroup including the spacer of 12 carbon atoms plus the histag ( $d=2.8$  nm). The thickness of the charged layer  $b$  depends linearly on the number of charged peptides ( $b=0.3$  nm per charged amino acid residue). A higher salt concentration of the electrolyte solution should result in a bigger screening of the charges, and thus not only in a smaller shift of the surface potential, but also in a less extended configuration of the peptides. Indeed, the sensor's response and the effective distance of the peptide both decrease with increasing salt concentration, as can be seen in Figure 2B. The mean distance—as well as the average distance between the charged peptides—is decreased, owing to the higher electrolyte screening ( $d=2.3$  nm and 0.1 nm per charged amino acid residue). This demonstrates that it is possible to determine quantitatively the charge and charge variations of small compounds by taking the Debye screening into account. Owing to electrolyte screen-

ing, the sensor's response is strongly dependent on the distance between the biomolecules and the sensor surface.

The effect of Debye screening on the detection of the protein binding to the membrane by their intrinsic charge was studied by the reversible binding of His-tagged GFP (green fluorescent protein) at physiological salt concentrations (140 mM KCl). Once the functional lipid headgroups were loaded with  $\text{Ni}^{++}$ , a buffer containing  $7 \mu\text{M}$  of protein was added. The surface potential, and thus the resistance of the nanometer thin silicon layer, shifts with the binding of the protein, as can be seen in Figure 3. To ensure conditions with constant electrolyte

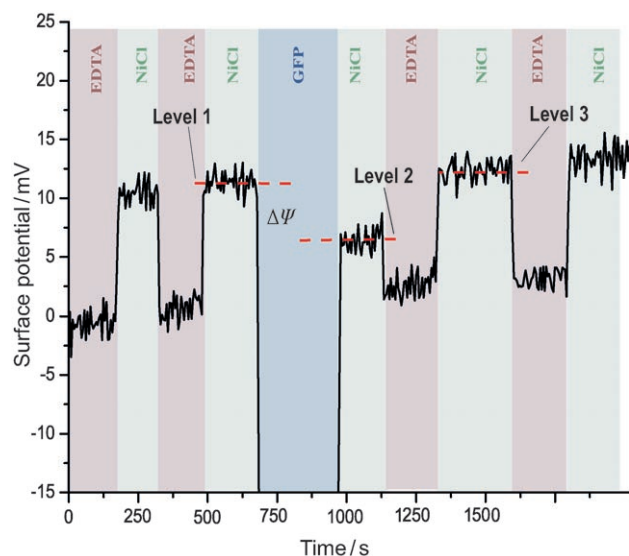


**Figure 3.** The binding of His-tagged GFP was detected at a physiological salt concentration of 140 mM ( $\kappa^{-1} = 0.7 \text{ nm}$ ) by measuring the resistance changes of the sensor device. Using prior calibration measurements, these resistance changes are related to changes in the surface potential. First,  $\text{Ni}^{++}$ -containing phosphate-buffered saline (PBS) buffer (1 mM) results in a charge variation of the NTA headgroups, which is reversible upon rinsing with an EDTA (50 mM) containing solution. The binding of the His-tagged GFP after preloading the NTA headgroup with  $\text{Ni}^{++}$  results in a shift in the surface potential. The specific signal can only be determined in presence of the same buffer solution and thus the surface potential difference ( $\Delta\Psi = 6 \text{ mV}$ ) between the levels marked as level 1 and level 2 can be attributed to the bound protein, which changes the effective surface charge density. The unbinding of the protein was achieved by rinsing with an EDTA containing PBS buffer, and the original surface potential was recovered. Differences between the signals marked as level 1 and level 3 are attributed to unspecific residual binding and were always lower than 10% of the specific binding signal.

concentrations, the buffer was exchanged with the standard  $\text{Ni}^{++}$ -containing buffer and only the sensor's signal in the presence of this buffer solution was analyzed for quantification of the sensor's response. The binding of GFP to the membrane results in a resistance shift corresponding to a change in surface potential of 6 mV. The protein was released from the membrane by applying an EDTA solution, and the surface potential prior to the binding of the protein was recovered, clearly demonstrating the specific and reversible binding of the protein.

The response of the sensor is concentration-dependent, as can be seen in Figure 4. Higher concentrations of GFP trigger the signal and result in an extended surface potential shift. Be-

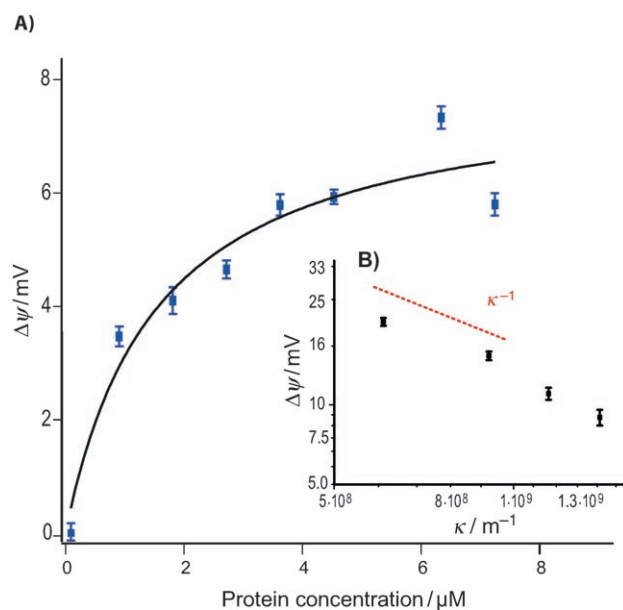


**Figure 4.** A) The binding of GFP to the membrane is concentration dependent, and the resulting response  $\Delta\Psi$  can be fitted by a Langmuir isotherm ( $K = 6 \times 10^5 \text{ M}^{-1}$ ). Error bars were determined from the measured electronic noise of the device. B) Keeping the concentration of GFP constant ( $7 \mu\text{M}$ ), the sensor signal upon the specific binding and unbinding of GFP was measured at different salt concentrations. The response shows a pronounced dependence on the screening length, as can be seen in the inset  $\kappa^{-1}$ , as indicated by the red line.

cause of the low concentration of functional lipids, a linear relation between the surface coverage and variations of the surface potential can be assumed. Thus, a Langmuir isotherm can be fitted to the obtained surface potential variations, yielding an equilibrium constant  $K$  of  $6.5 \times 10^5 \text{ M}^{-1}$ , in very good agreement with literature values.<sup>[25]</sup> The potential of this sensor method, in terms of determining reliable and absolute values, is demonstrated by performing the measurements using different lots of sensor chips (Figure 4). Differences in the defect densities in the lipid membrane do not seem to affect the measured response.

In this series of experiments, an observed detection limit of  $1 \mu\text{M}$  was set by the density of functional lipids and the screening effects of the physiological electrolyte solution used (140 mM KCl). The absolute resolution limit was set by the intrinsic sensor noise, which depends mainly on the quality of the oxide layer and the biofunctionalization. At the functional surface group density used, typical noise levels enable the detection of unscreened charge differences of about  $0.001 e^- \text{ nm}^{-2}$ , and can be optimized by semiconductor technologies, noise filtering, and functionalization.

GFP has 26 positively and 33 negatively charged amino acid side groups at pH 7. These charged amino acid residues are unevenly distributed over its whole structure, which makes it

impossible to predict a simple relationship between the surface potential variation and the net charge of the protein.<sup>[26]</sup> However, the detection of the complex charge distribution of the protein still has to be sensitive to the screening effects in the electrolyte solution. Indeed, the variations in the salt concentration result in a significant dependence in the sensors response to the Debye screening length  $\kappa^{-1}$  (Figure 4B). The binding of a constant GFP concentration of 7  $\mu\text{M}$  to the sensor surface results in a significantly higher sensor response at low ionic strengths. Varying the salt concentration so that the Debye screening length is  $\kappa^{-1}=0.75\text{--}1.61$  nm results in a two-fold higher surface potential. Thus, much smaller quantities of protein are detectable at lower salt concentrations. The sensor signal was almost linearly dependent on the Debye screening length. As the size of the protein is bigger than typical screening lengths, the observed dependence of the sensor's response on the screening length can mainly be attributed to the inhomogeneous charge distribution of the protein. More refined theoretical models have to be developed to relate the sensor's response to the complex electrostatic properties of proteins.

We have shown that biofunctionalized SOI resistors are well-suited to detect biomolecular interactions in real time, enabling the quantitative detection of the intrinsic charges of small peptides or proteins. Taking into account screening effects demonstrates the possibilities of field-effect devices for biosensing applications. We show that the distance of the analyte to the surface of the biosensing field-effect device is a critical parameter, which has to be tightly controlled in future applications. The introduced biosensing SOI resistor is able to distinguish a charge difference down to single charge variations in electrolyte solutions. The possibility of detecting low molecular mass molecules could prove to be extremely helpful for drug-screening assays. The presented functionalization of the sensor with NTA lipids is very promising for the specific immobilization of His tagged antibodies or receptor proteins. The incorporation of other functional lipids or even membrane proteins into lipid bilayers has been demonstrated in other systems, and should easily be transferred to the presented device. As the SOI resistor was built by standard semiconductor technology, the parallization and miniaturization for highly sensitive, quantitative, high-throughput applications can, in principle, be realized.

## Materials and Methods

**SOI-Based Thin-Film Resistor:** The production process of the bare surface sensors and the detailed characterization of the measured response curves in electrolyte solution is described elsewhere.<sup>[17]</sup> The 30 nm thick conducting silicon layer of the SOI substrate was structured by standard lithography. Isolation of all electrical contacts from the aqueous solution was achieved by bonding the sensor into a chip carrier with an ultrasound bonder and encapsulating the bond wires, metallization, and contact pads with silicon rubber. The sheet resistance was determined in a 4-point geometry utilizing a Hallbar: A current was applied with a Keithley K2400 source-meter between the source and drain, and the voltage drop between two adjacent contacts was measured continuously. The back-gate voltage was applied with an Agilent E3647A voltage

source. Long-term drift of the signal was subtracted prior to analysis. The potential of the electrolyte was controlled using an Ag/AgCl reference electrode (METROHM, Germany) immersed into the electrolyte, which also was used for calibration measurements. The calibration measurements in electrolyte solutions were used to relate the surface potential of the passivated sensor device to the sheet resistance. The sensor and the reference electrode were mounted into a microfluidic chamber ensuring flow conditions for a rapid exchange of analytes at the interface.<sup>[17]</sup> The sensitive area of the device is huge (80  $\mu\text{m}\times 80 \mu\text{m}$ ) in comparison to the average area per functional DOGS-NTA lipid (65  $\text{\AA}^2$ ). The charge-carrier concentration of the conducting silicon layer was controlled by applying a back-gate voltage ( $U_{\text{bg}}=25$  V) and thus tuning the sensitivity of the sensor device.<sup>[27]</sup> Typical conductivities of the conducting layer were 25  $\text{k}\Omega\text{square}^{-1}$ .

**Surface Functionalization:** The bare surface sensors were passivated by the covalent binding of ODTMS (octadecyltrimethoxysilane) to the oxide surface, resulting in a hydrophobic surface. The contact angle changed from  $<10^\circ$  to approximately  $90^\circ$  on the hydrophobic surfaces, and the thickness of the silane layer was measured with ellipsometry to be 1.5 nm, indicating a monolayer. After the hydrophobization, the sensor chips were encapsulated and plugged into the measurement setup. The flowchamber was put on top of the sensors for the application of different electrolyte solutions.

The desired amounts of lipids in chloroform solution were mixed in a glass flask to yield a total lipid concentration of 1  $\text{mg mL}^{-1}$  solution. Afterwards, the solvent was evaporated under nitrogen, and the glass was stored under vacuum over night. The dried lipids were dissolved in pure ethanol and injected into the chamber mounted on the sensor. The spontaneous formation of the lipid monolayer was initiated by rinsing the chamber with degassed standard buffer at a flow rate of 10  $\mu\text{L s}^{-1}$ . A peristaltic pump (ISMATECH, Germany) applied this flow for 10 s, followed by a rest time of 90 s. After approximately 2 h, the chamber was rinsed with buffer to remove all residual lipids and ethanol. In all experiments, a mixture of DMPC and cholesterol was used as the matrix lipid, and 5% DOGS-NTA (1,2-dioleoyl-sn-glycero-3-[[N(5-amino-1-carboxypentyl)iminodiacetic acid]succinyl) was added.

In all experiments, standard PBS buffer (pH 7.5) with varying concentrations of KCl was used. The standard  $\text{Ni}^{++}$  buffer contained an additional 1 mM NiCl. The EDTA buffer contained 90 mM KCl and 50 mM EDTA. Both  $\text{Ni}^{++}$  and EDTA containing buffers were equilibrated prior to the binding experiments: The buffers were titrated with KCL until the sensor's response to small variations in the electrolyte concentrations between the  $\text{Ni}^{++}$  and EDTA buffer was no longer detectable.

## Acknowledgements

*The project was funded by the DFG within the SFB 563 TP B12. The support of the "Fonds der Chemischen Industrie" is gratefully acknowledged. M.G.N. was supported by the Studienstiftung des deutschen Volkes. We thank Roland Netz and M. Tanaka for many fruitful discussions, and G. Abstreiter for the continuous support and the generous access to the clean-room facilities of the Walter Schottky Institut. We also thank Karin Buchholz and Marc Tornow for support with the Silicon technology.*

**Keywords:** biosensors · field effect · peptides · proteins · thin-film resistor

- [1] L. Hood, L. J. R. Heath, M. E. Phelps, B. Y. Lin, *Science* **2004**, *306*, 640–643.
- [2] Y. Fang, A. G. Frutos, J. Lahiri, *J. Am. Chem. Soc.* **2002**, *124*, 2394–2395.
- [3] D. S. Wilson, S. Nock, *Angew. Chem.* **2003**, *115*, 510–517; *Angew. Chem. Int. Ed.* **2003**, *42*, 494–500.
- [4] P. K. Tan, T. J. Downey, E. L. Spitznagel, P. Xu, D. Fu, D. S. Dimitrov, R. A. Lempicki, B. M. Raaka, M. C. Cam, *Nucleic Acids Res.* **2003**, *31*, 5676–5684.
- [5] R. L. Rich, D. G. Myszka, *Curr. Opin. Biotech.* **2000**, *11*, 54–61.
- [6] J. Fritz, M. K. Baller, H. P. Lang, H. Rothuizen, P. Vettiger, E. Meyer, H. J. Guntherodt, C. Gerber, J. K. Gimzewski, *Science* **2000**, *288*, 316–318.
- [7] *Bioelectronics* (Eds.: I. Willner, E. Katz), Wiley-VCH, Weinheim, **2005**.
- [8] P. Bergveld, *Sens. Actuators B* **2003**, *88*, 1–20.
- [9] W. S. Yang, R. J. Hamers, *Appl. Phys. Lett.* **2004**, *85*, 3626–3628.
- [10] F. Patolsky, G. F. Zheng, O. Hayden, M. Lakadamyali, X. W. Zhuang, C. M. Lieber, *Proc. Natl. Acad. Sci. USA* **2004**, *101*, 14017–14022.
- [11] J. Fritz, E. B. Cooper, S. Gaudet, P. K. Sorger, S. R. Manalis, *Proc. Natl. Acad. Sci. USA* **2002**, *99*, 14142–14146.
- [12] F. Pouthas, C. Gentil, D. Cote, G. Zeck, B. Straub, U. Bockelmann, *Phys. Rev. E* **2004**, *70*, 031906.
- [13] F. Uslu, S. Ingebrandt, D. Mayer, S. Bocker-Meffert, M. Odenthal, A. Ofenhausser, *Biosens. Bioelectron.* **2004**, *19*, 1723–1731.
- [14] Y. Cui, Q. Q. Wei, H. K. Park, C. M. Lieber, *Science* **2001**, *293*, 1289–1292.
- [15] J. Hahn, C. M. Lieber, *Nano Lett.* **2004**, *4*, 51–54.
- [16] Y. L. Bunimovich, G. L. Ge, K. C. Beverly, R. S. Ries, L. Hood, J. R. Heath, *Langmuir* **2004**, *20*, 10630–10638.
- [17] M. G. Nikolaidis, S. Rauschenbach, S. Luber, K. Buchholz, M. Tornow, G. Abstreiter, A. R. Bausch, *ChemPhysChem.* **2003**, *4*, 1104–1106.
- [18] E. Sackmann, *Science* **1996**, *271*, 43–48.
- [19] M. Tanaka, E. Sackmann, *Nature* **2005**, *437*, 656–663.
- [20] L. Schmitt, C. Dietrich, R. Tampe, *J. Am. Chem. Soc.* **1994**, *116*, 8485–8491.
- [21] H. Hillebrandt, M. Tanaka, E. Sackmann, *J. Phys. Chem. B* **2002**, *106*, 477–486.
- [22] J. G. Altin, F. A. J. White, C. J. Easton, *BBA—Biomembranes* **2001**, *1513*, 131–148.
- [23] I. T. Dorn, K. R. Neumaier, R. Tampe, *J. Am. Chem. Soc.* **1998**, *120*, 2753–2763.
- [24] R. R. Netz, *Phys. Rev. E* **1999**, *60*, 3174–3182.
- [25] L. Nieba, S. E. NiebaAxmann, A. Persson, M. Hamalainen, F. Edebratt, A. Hansson, J. Lidholm, K. Magnusson, A. F. Karlsson, A. Pluckthun, *Anal. Biochem.* **1997**, *252*, 217–228.
- [26] D. Murray, A. Arbuzova, B. Honig, S. McLaughlin in *Current Topics in Membranes: Peptide-Lipid Interactions* (Eds: S. Simon, T. McIntosh), Academic Press, London, **2002**.
- [27] M. G. Nikolaidis, S. Rauschenbach, A. R. Bausch, *J. Appl. Phys.* **2004**, *95*, 3811–3815.

Received: August 30, 2005

Published online on January 11, 2006